



## A Low Profile Four-Port MIMO Array Antenna with Defected Ground Structure for 5G IoT Applications

Ouafae Elalaouy<sup>1\*</sup>, Mohammed El Ghzaoui<sup>2</sup>, Jaouad Foshi<sup>3</sup>

<sup>1,3</sup> Moulay Ismail University, Faculty of Sciences and Techniques, Errachidia, Morocco  
E-mail: [ou.elalaouy@edu.umi.ac.ma](mailto:ou.elalaouy@edu.umi.ac.ma)

<sup>2</sup> Faculty of Sciences Dhar Elmahraz, Sidi Mohamed Ben Abdellah University, Fez, Morocco

Received: January 16, 2023

Revised: March 27, 2023

Accepted: April 10, 2023

**Abstract**—The overwhelming demand for high-data-rate applications and low latency, which are prerequisites for multimedia content, are propelling technological advancements toward 5G communication networks. To acquire the intended 5G requirements and further encapsulate many application areas, a number of technologies has been implemented including millimeter waves and multiple input multiple output (MIMO) systems. One of the primary limitations in creating small MIMO antennas is the presence of inter-element mutual coupling. To cope with the non-desired mutual coupling, this work embodies a defected ground structure (DGS) MIMO antenna operating in a millimeter-wave 5G band. The proposed MIMO array antenna comprises four ports with eight identical patches. It has a total surface area of 50x60 mm<sup>2</sup>, and is printed on FR4 epoxy substrates with a 4.4 dielectric constant. The bandwidth of the presented structure is extended thanks to the incorporation of slots. The simulation results demonstrate a wide bandwidth covering from 26.9 to 29.3 GHz, and that owing to the DGS, the mutual coupling is alleviated. Subsequently, a high level of isolation (greater than -27 dB), and an ultimate peak gain of 5.525 dBi are reached over the resonance bandwidth. Moreover, investigation of the MIMO diversity performance shows the following parameters: the envelope correlation coefficient (ECC) < 0.0003, diversity gain (DG) > 9.999 dB, and the total active reflection coefficient (TARC) < -10 dB in the operating band. Additionally, the antenna is found to cover the band allocated to 5G in both USA (27.5-28.35 GHz) and Japan (27.5-28.28 GHz). Based on the obtained results, the proposed MIMO array antenna is useful for application in both 5G band handsets and future IoT applications.

**Keywords**— MIMO antenna; 5G; IoT; Defected ground structure; Gain; Envelope correlation coefficient.

### 1. INTRODUCTION

Multiple input multiple output (MIMO) technology has witnessed rapid development within the field of mobile communication [1-3]. The 5G communication system is expected to handle the growth in forecasted data traffic by embracing the MIMO antenna as an emerging key technique. Due to multipath fading, researchers are highly stressing the use of many antennas both for transmitting and receiving purposes. This should be done to enhance the data rate and to provide decent link reliability through spatial diversity and spectral efficiency via multiplexing techniques. Although MIMO is utilized to overcome various drawbacks, it still suffers from mutual coupling, especially among the closest spaces. Therefore, a number of approaches have been adopted to solve this hitch namely defected ground structure and antenna separation.

To realize MIMO antenna that can be used for smartphones, multi-antennas have been proposed in the literature [4-10]. A 4-port UWB MIMO antenna system has been suggested in

\* Corresponding author

[4]. This antenna has a wide bandwidth along with high gain. In [5], a MIMO antenna with a high degree of isolation is designed for smartwatch applications. In [6], MIMO antenna operating at 28/38 GHz has been proposed for 5G smartphones. The suggested antenna offers a peak gain of 9 dBi. In [7], Aghoutane et al. have proposed a MIMO antenna for 5G applications. The authors used a new geometry of ground plan with array elements to form the MIMO antenna. The proposed antenna has dual-band properties, it covers the two bands (27.50-28.35 GHz) and 37 GHz (37-37.6 GHz). In [8], a MIMO antenna array has been introduced for 5G applications. The antenna covers the band (25.5-29.6 GHz) and the antenna gain about 8.3 dBi. In [9], a slot patch antenna has been reported for 28/38 GHz bands. This antenna is dual-band and offers a maximum peak gain of about 9 dBi at 28 GHz. In [10], a new shape is given to the antenna. The proposed MIMO antenna with an end-launch connector model for 5G Millimeter Wave Mobile Applications was used. The suggested antenna in [11] has an impedance bandwidth of 2.6 GHz (27.4–30.0 GHz) and 3.3 GHz (36.7–40.0 GHz). Besides, the antenna allows peak gains of 18 and 14.5 dBi at 28.5 and 38.8 GHz, respectively. The experiments carried out in [12-15] along with the above-cited references helped us to have a clear picture of the status of antenna for 5G applications as well as the design requirements for the implementation of printed antennas for mobile applications. One of the primary limitations in creating small MIMO antennas is the presence of inter-element mutual coupling. Different techniques to hamper the mutual coupling has been proposed including the Defect Ground Structure (DGS). Several researchs related to this issue have been reported in the literature [16-20] as indicated in Table 1, these MIMO antennas offer a narrow bandwidth. Thus, the aim of this work is to further enhance the bandwidth as well as the gain and isolation.

In the current study, a four-port MIMO antenna is proposed making use of defected ground structure to cope with the non-desired mutual coupling. As indicated in Table 1, the suggested MIMO antenna operates at 27.7 GHz and has a bandwidth of 2.4 GHz (26.9–29.5 GHz) with a peak gain of 5.25 dBi. In addition, it provides an isolation of less than -27 dB. Besides, it remains within the allowed standards in terms of ECC, which is less than 0.003, and the DG, which is very close to 10 dB. As a result, the proposed MIMO array antenna can be considered a capable mm-wave antenna for upcoming 5G networks.

Table 1. Comparison of the proposed with existing MIMO antennas.

Ref.	Dimensions [mm <sup>3</sup> ]	Bandwidth [GHz]	Isolation [dB]	Gain [dBi]	ECC
[4]	75 × 150 × 1.6	2.6–10.2 (118%)	>16	6	<0.007
[5]	π × 182 × 7	2.4–2.49 (3.6%)	>20	3.5	-
[6]	21.6 × 20 × 0.25	25.5–28.9 (12.5%) 37–38.4 (3.7%)	>38	9	<0.0085
[7]	43.611 × 43.611 × 0.4	27.4–28.6 (4.2%) 36.7–38.5 (4.8%)	>20 >30	7.9 13.7	<0.00025 <0.00035
[8]	30 × 35 × 0.76	25.5–29.6 (14.8%)	>17	8.31	<0.01
[16]	26 × 26 × 8	5.61–5.9 (5%)	>18.2	1.61	<0.02
[17]	42.837 × 34.4 × 0.8	5.6–5.95 (6%)	>37.5	-	<0.0001
[18]	21.6 × 20 × 0.25	3–3.5 (15%)	>38	4.583	-
[19]	16 × 12 × 0.787	5.21–5.5 (5.4%)	>18	2.25	<0.02
[20]	74 × 74 × 0.015	5.82–5.94 (2%)	>34	7.68	<0.001
Proposed	50 × 60 × 1.6	26.9–29.3 (8.5%)	>27	5.25	<0.0001

## 2. DESIGN FLOW

The proposed four-port MIMO is modeled and simulated using the FEM solver in the HFSS Microwave Studio suite. We have chosen to use the automatic meshing feature to ensure that the simulation accurately captures the electromagnetic fields around the waveguide. The design process involved three main steps leading up to the proposed MIMO structure shown in Fig. 1. A single resonator is designed in the first step. In the second, a two-element array antenna is built. Finally, the latest design is extended to four-element MIMO. Therefore, the sections that follow will endeavor to explore the design evolution from a single element to the suggested MIMO configuration.

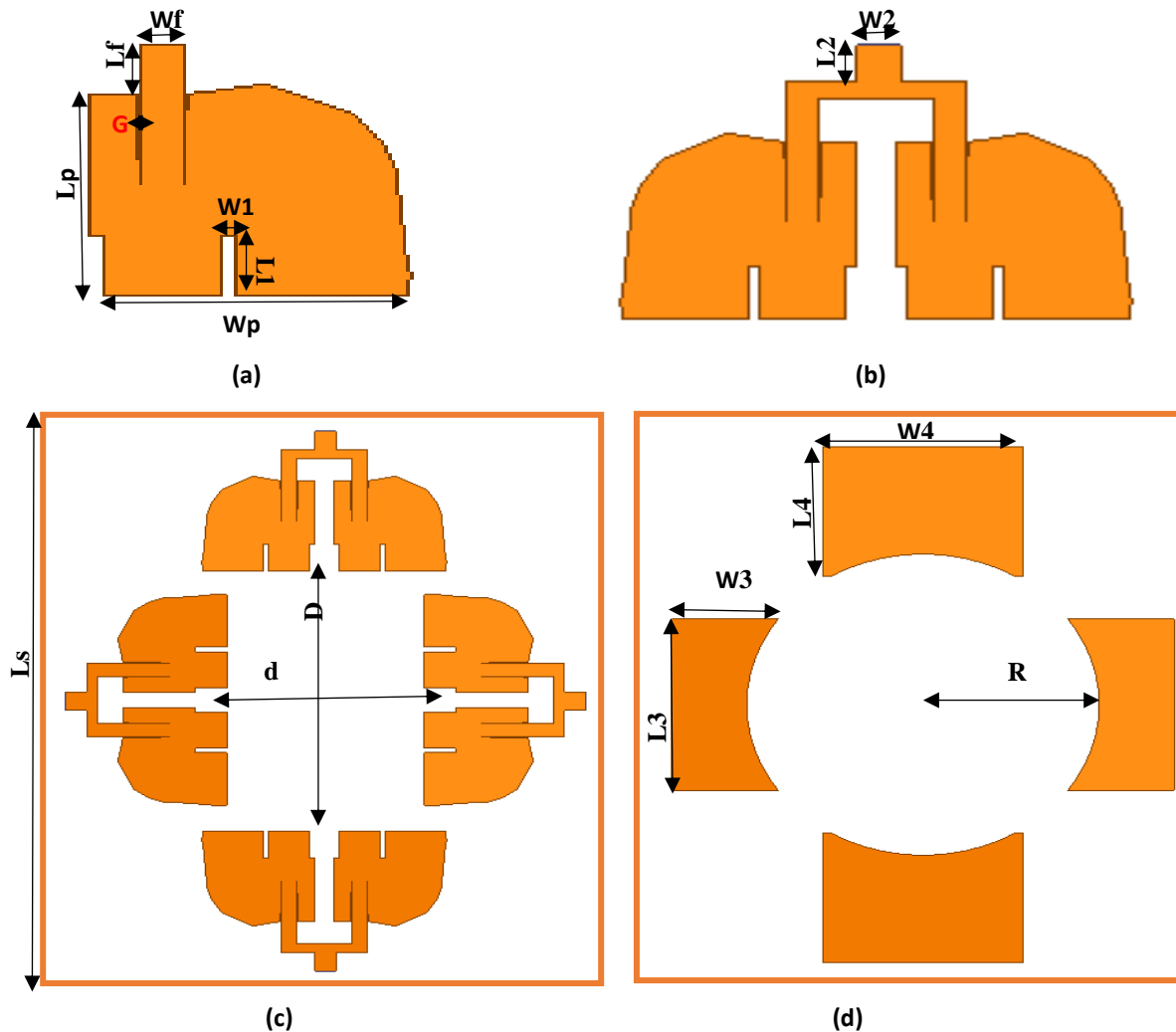


Fig. 1. MIMO antenna geometry: a) single patch; b) 2-element array and 4-port MIMO; c) top plane; d) back plane.

### 2.1. Single Element Antenna

Design flow of the proposed single input single output (SISO) has been initiated from a rectangular patch antenna. The antenna and feed line dimensions were calculated using the conventional equations [21]. The proposed single patch shown in Fig. 1 was obtained by implementing staggered modifications to the initial rectangular patch, which are adding rectangular slots and etching the rectangular patch. The final version of the single antenna was used to develop the MIMO antenna. The structural dimensions of the single patch are listed in Table 2.

Table 2. Parameters of the proposed MIMO antenna.

Parameter	Value [mm]	Parameter	Value [mm]
Ls	50	Lp	10
Ws	60	Wp	10
D	29	Lf	2.5
D	19	Wf	1.5
L1	3	L3	20
W1	0.5	W3	15
L2	2	L4	15
W2	2	W4	20
H	1.6	R	17.5
G	0.5		

## 2.2. Two-Element Array

The second stage of the construction involved employing a T-junction power divider to join two identical Single Input Single Output (SISO) patches into the two-element array. The parallel feed network is employed to stimulate the configured array. The impedance of the main feed line is adjusted to 50 ohms for optimal performance, while the branch lines in the network are matched to an impedance of 100 ohms to ensure efficient power transfer. The two-element array's structural arrangements and its feeding network are shown in Fig. 2(b).

## 2.3. MIMO Antenna

To reach the final version of the MIMO antenna, the aforementioned developed array antenna was utilized as displayed in Fig. 1. Eight identical patch antennas constitute the top layer. The backplane consists of a defected ground structure to mitigate the mutual coupling. The whole design was built on a cheap FR4 epoxy substrate with a thickness of 1.6 mm, dielectric constant  $\epsilon_r = 4.4$ , and resonant frequency  $f_r = 27.7$  GHz.

One can notice from Fig. 2 that the presented MIMO operates in 26.9-29.3 GHz with a good impedance matching of -14.2 dB and a high isolation. Furthermore, The MIMO antenna achieves 5.25 dBi, in both American and Japanese bands that are respectively 27.5-28.35 GHz and 27.5-28.28 GHz, as shown in Fig. 4.

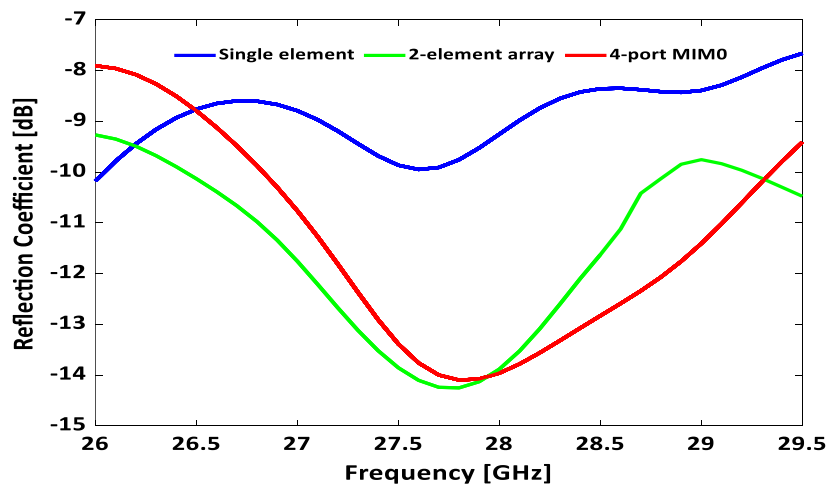


Fig. 2. Simulated reflection coefficient of single element, 2-element array and 4-port MIMO.

### 3. RESULTS AND DISCUSSION

#### 3.1. Reflection Coefficient

The comparison of the simulated reflection coefficient  $S_{11}$  versus the frequency plots of the single-element antenna, the 2-element array, and the suggested MIMO antenna is displayed in Fig. 2. It is contemplated from Fig. 2 that the single antenna provides poor matching characteristics as it does not assert  $S_{11} < -10$  dB. However, the 2-element array antenna befits the desired reflection coefficient criterion as it is lower than -10 dB at the band ranging from 26.5 GHz to 28.8 GHz. As a result, the proposed MIMO antenna is designed. It is clearly visible that the MIMO system exhibits a wide bandwidth of 2.4 GHz from 26.9 GHz to 29.3 GHz along with a return loss of -14 dB at 27.7 GHz. Thus, the constructed scheme can cover the mm-wave 5G spectrum mainly at 27.7 GHz.

#### 3.2. Isolation

MIMO array antenna systems possess the inherent ability to increase the gain. Adversely, mutual coupling tends to occur among the MIMO antenna elements, which alters the current distribution and deteriorates the antenna's isolation performance. Broadly, the simple way to alleviate this issue is to keep the space between the antenna elements at least at  $\lambda_0/2$ . Nonetheless, this causes an increase in the MIMO structure size. Thus in this work, an effective as well as simple method of decoupling is deployed. Fig. 3 displays the isolation characteristics of the reported MIMO antenna. From Fig. 3, it is clearly visible that the isolation of the MIMO structure is less than -23 dB when using a total ground whereas the isolation with DGS is better than -27 dB. The obtained isolation will ensure that the desired signal is transmitted with minimal interference from other signals or noise, leading to improved signal quality, increased range, enhanced reliability, improved security, and better coexistence with other systems.

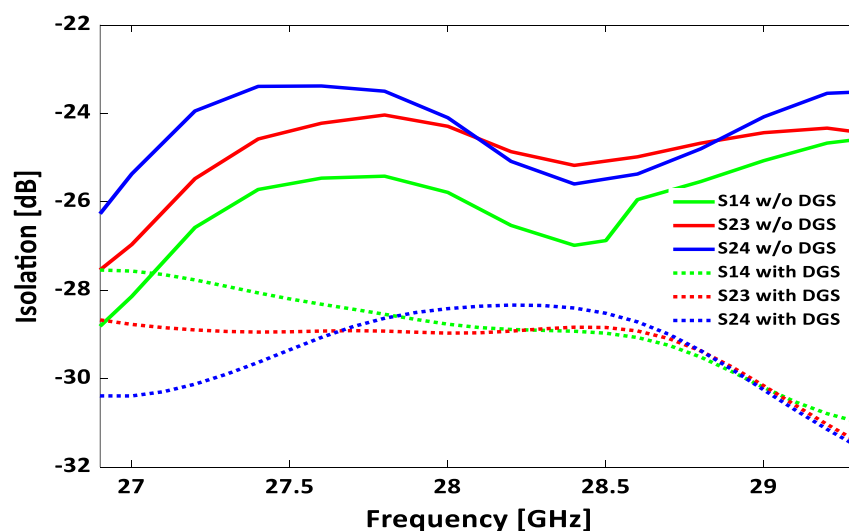


Fig. 3. Simulated isolation of the 4-port MIMO with and without DGS.

#### 3.3. Gain

To illustrate the antenna performance through each design stage, we moved from the single element to the final proposed MIMO design in terms of antenna gain, which is highlighted in Fig. 4. It seems, then, evident to claim that the single antenna achieves a peak

gain of 3.36 dBi. Additionally, it is seen that the antenna gain for the 2-element array design is noticeably better than the single antenna, which has a peak gain of 4.2 dBi. Without the DGS, the MIMO antenna's peak gain throughout the essential band is almost identical to the antenna array structure's gain. However, when DGS technique is used, as indicated in Fig. 5, the peak gain increases to about 5.25 dBi with 27.7 GHz over the entire operating bandwidth including the American and Japanese bands that are respectively 27.5-28.35 GHz and 27.5-28.28 GHz. It can be drawn that the Defected Ground Structure (DGS) can have a positive effect in microwave components. In terms of gain, DGS structures can improve gain by increasing the efficiency of microwave components through improved impedance matching, reduced crosstalk, and radiation. Thus, the reached structure will be able to transmit or receive more power in a particular direction than an antenna with a lower gain. This is achieved by directing the antenna's radiation pattern more toward the desired direction and reducing it in other directions. This can be particularly useful in long-distance communication systems, where the signal may need to travel a significant distance and encounter obstacles that can weaken or interfere with the signal.

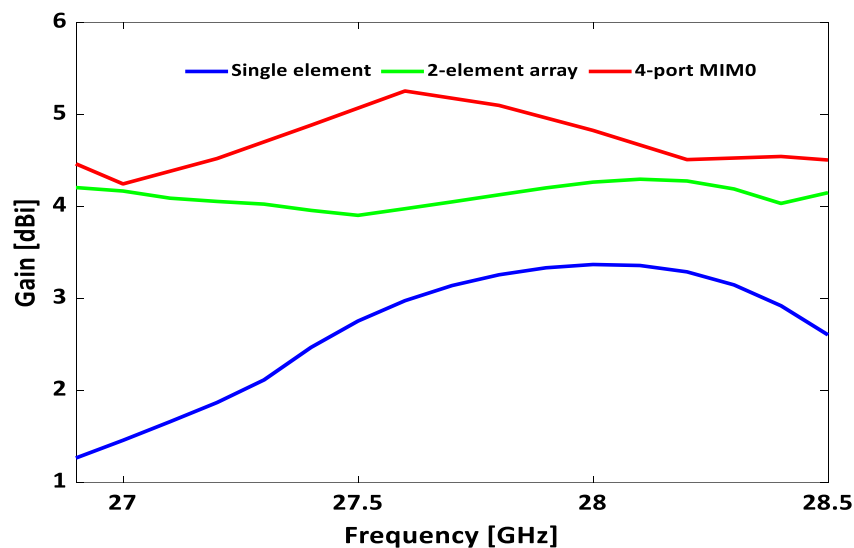


Fig. 4. Simulated gain of single element, 2-element array and 4-port MIMO.

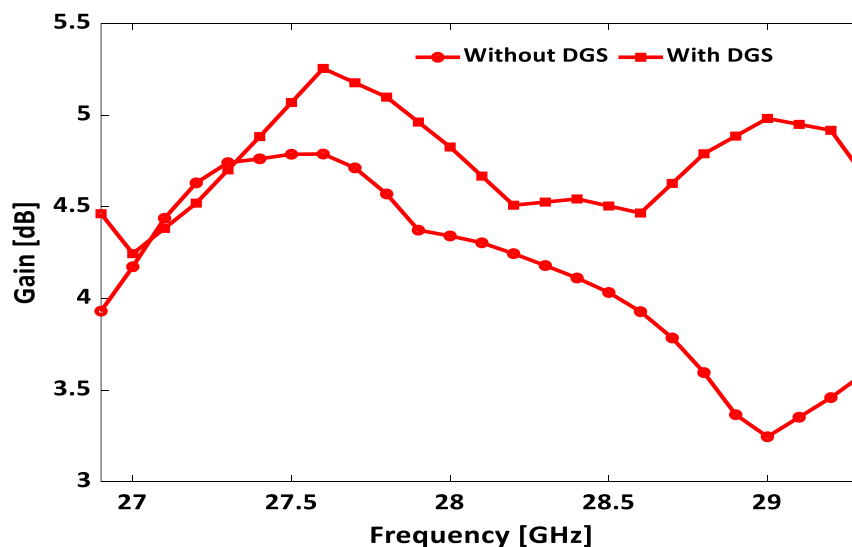


Fig. 5. Simulated gain of the 4-port MIMO with and without DGS.

### 3.4. Radiation Efficiency

The radiation efficiency of the designed MIMO antenna is shown in Fig. 6. It can be noticed that the proposed structure reached approximately 99% at the resonating frequency of 27.7 GHz. Furthermore, the radiation efficiency values lay between 95% and 99%.

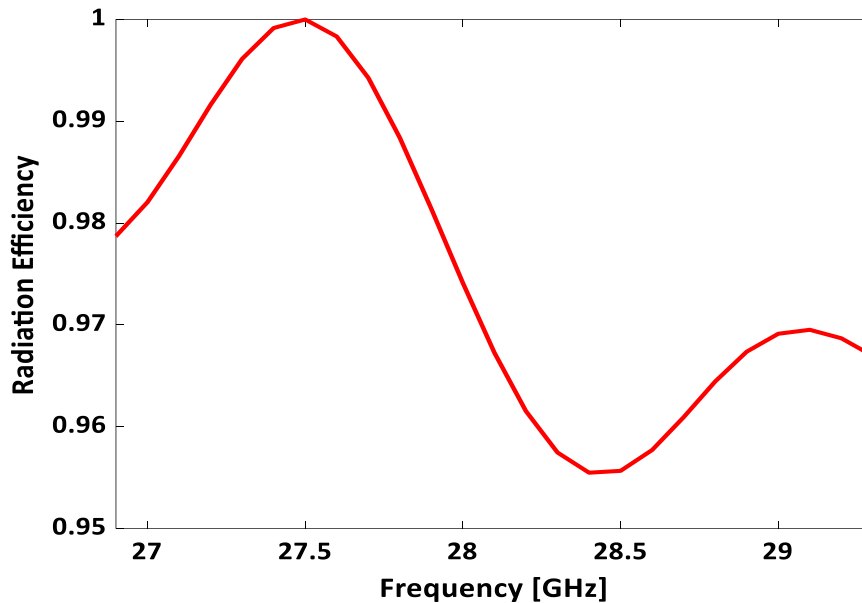


Fig. 6. Simulated radiation efficiency of the 4-port MIMO.

The study of increasing elements among MIMO antennas is much valued as it offers a detailed understanding of the enhancement of the characteristics parameters. The single-element antenna does not provide satisfactory results in terms of impedance matching as well as gain. Furthermore, a configuration array is built to increase gain and enhance the bandwidth for the proposed 5G applications. The two-element array antenna has a bandwidth of around 2 GHz (26.5–28.5) at 27.7 GHz with a low return loss of roughly 14.33 dB. Compared to a single-element array, the gain provided by the two-element array is slightly increased. However, the array antenna's lower gain is insufficient to meet 5G requirements. Yet, it provides satisfactory results in terms of bandwidth. For the sake of improving antenna radiation, a four-port MIMO antenna array is projected for 5G IoT applications. It can be deduced that as far as elements are added, the impedance matching, as well as the gain, were further improved due to the creation of additional resonant modes or stopbands. This occurs because the added elements modify the effective permittivity of the ground plane and create new resonances, which in turn can enhance the efficiency of the component, reduce unwanted reflections and crosstalk and lead to a broader bandwidth. Furthermore, employing a partial ground and incorporating the circle shape slot on the bottom layer provides satisfactory isolation along with sufficient gain, which is due to the inherent characteristics of DGS as it creates a high impedance surface, which acts as a reflector for electromagnetic waves at certain frequencies. This reflection reduces the coupling between different parts of the circuit and improves the isolation. Table 3 shows that the considered MIMO array antenna outperforms the single and the 2-element array in terms of bandwidth and gain which are enhanced respectively to 2.4 GHz and to 5.25 dBi.

Table 3. Performance of single 2-elements array and the proposed MIMO antenna.

Structure	Bandwidth [GHz]	S11 [dB]	Peak gain [dBi]
Single element	–	–	3.36
2 elements array	[26.5 – 28.5] = 2	-14.2	4.2
MIMO with DGS	[26.9 – 29.3] = 2.4	-14	5.25

#### 4. MIMO PERFORMANCE METRICS

It is compulsory to calculate the MIMO diversity performance through the measurement of the envelope correlation coefficient ECC, the diversity gain DG, the channel capacity loss CCL, the total active reflection coefficient TARC, and the mean effective gain MEG to assess the 4-port MIMO effectiveness. The next sections will give the thorough analyses for each of these parameters.

##### 4.1. Envelope Correlation Coefficient and Diversity Gain

A key parameter known as ECC is used to measure the correlation among the patch antennas. ECC should be lower than 0.05 to have a tolerable radiation diversity. The envelope correlation coefficient for a MIMO configuration can be calculated with the help of the S-parameters in accordance with Eq. (1) [7].

$$ECC = \frac{|\sum_{n=1}^N S_{i,n} S_{n,j}^*|^2}{\prod_{k=(i,j)} [1 - \sum_{n=1}^N S_{k,n} S_{n,k}^*]} \quad (1)$$

The  $i$ th antenna,  $j$ th antenna, and the total number of antennas are denoted by  $i$ ,  $j$ , and  $N$ .

The DG is a significant additional factor to judge the MIMO performance. It is expressed as an increase in the signal to interference level and can be calculated as [7]:

$$DG = 10\sqrt{1 - ECC^2} \quad (2)$$

The simulated ECC and DG plots for the proposed MIMO antenna are depicted in Fig. 7. From our observation, we have noticed that the ECC values gratify the standard requirements of  $<0.5$ . It remains below 0.0003 over the entire bandwidth. Besides, the DG is clearly getting closer to the threshold value of 10 dB within the operating bandwidth. Since the ECC values are below the threshold value and the DG is almost nearly at 10 dB across the whole bandwidth, the proposed MIMO antenna has proven to be an aspiring contender for 5G communication networks.

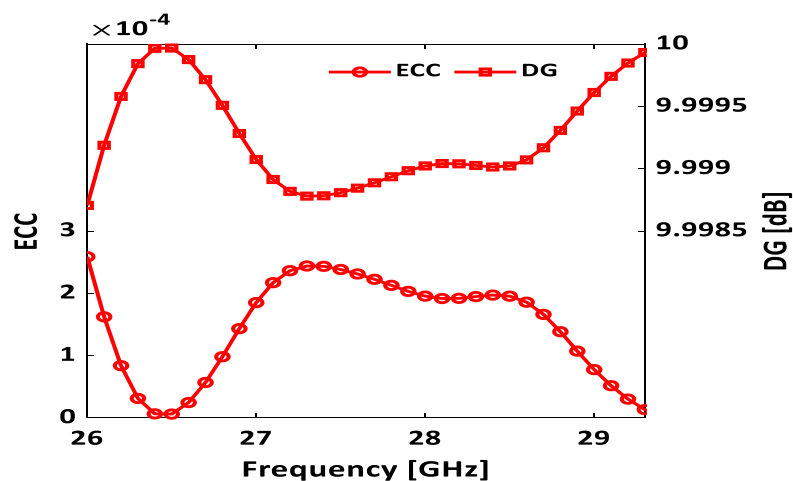


Fig. 7. Simulated ECC for the 4-port MIMO antenna.

### 4.2. Channel Capacity Loss

CCL plays a crucial role as it increases with the rise in the number of antennas within a MIMO system. CCL assesses the absolute limit at which a signal may be transmitted across a communication medium without suffering any loss. It is computed by making use of Eq. (3) [7]. The obtained CCL values are spotted in Fig. 8. It can be clearly seen, that the CCL values are less than the ideal value of 0.4 bits/s/Hz from 27 to 29 GHz.

$$CCL = -\log_2 \det(S) \tag{3}$$

where S is given by:

$$S = \begin{bmatrix} \alpha_{11} & \alpha_{12} & \alpha_{13} & \alpha_{14} \\ \alpha_{21} & \alpha_{22} & \alpha_{23} & \alpha_{24} \\ \alpha_{31} & \alpha_{32} & \alpha_{33} & \alpha_{34} \\ \alpha_{41} & \alpha_{42} & \alpha_{43} & \alpha_{44} \end{bmatrix}$$

where  $\alpha_{ii} = 1 - \sum_{j=1}^n |S_{ij}|^2$  And  $\alpha_{ii} = S_{ij}^* S_{ij} + S_{ji}^* S_{ij}$ .

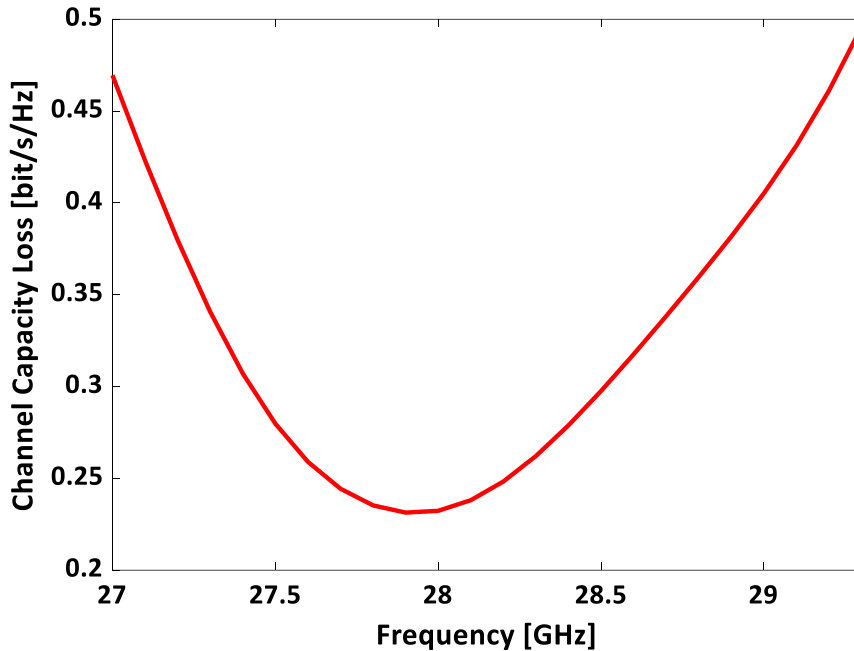


Fig. 8. Simulated CCL for the 4-port MIMO antenna.

### 4.3. Total Active Reflection Coefficient

TARC takes into account random signal combinations between ports in addition to mutual coupling. TARC is important to determine frequency bandwidth and radiation performance while using MIMO antennas. The TARC can be calculated using the formula below [7].

$$TARC = \sqrt{\frac{\sum_{i=1}^N |S_{i1} + \sum_{m=2}^N S_{im} e^{j\theta_{m-1}}|^2}{N}} \tag{4}$$

Fig. 9 displays the simulated TARC findings for input signals with phase changes of 60°, 90°, and 180°. It can be seen that the three curves are similar and are less than -8 dB within the essential operating band, demonstrating the satisfactory performance of the proposed system for 5G systems.

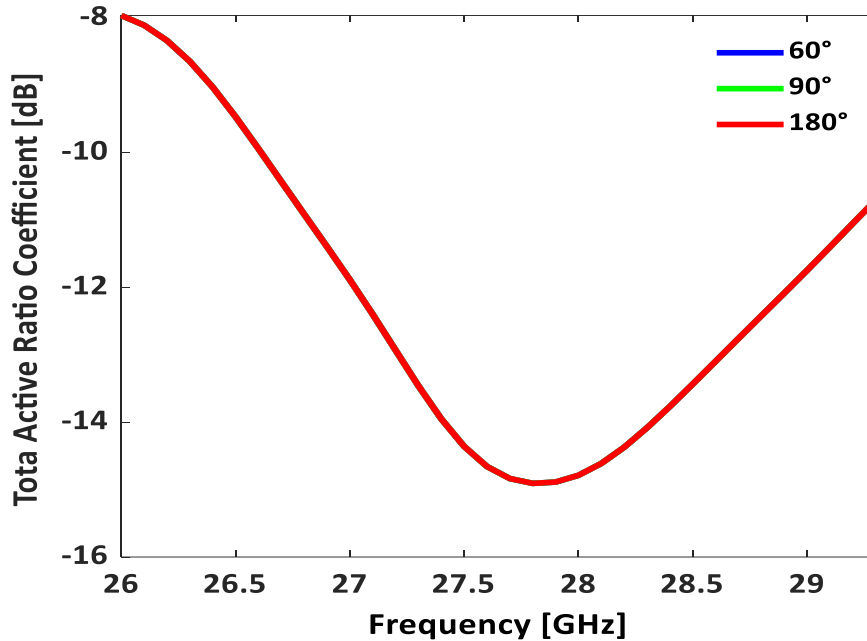


Fig. 9. Simulated TARC for the 4-port MIMO antenna at 60°, 90° and 180°.

#### 4.4. Mean Effective Gain

MEG provides the average accepted power in a multi-path channel. The standard MEG values should be between -4 dB and -3 dB to attain satisfactory performance. It is computed by the use of the below formula [7].

$$MEG = 1 - \sum_{j=1}^N |S_{ij}|^2 \quad (5)$$

Table 3 demonstrates the MEG parameter. This makes clear the idea that the proposed MIMO design provides MEG values that are very close to 3 dB at the entire bandwidth. Hence, the proposed structure gives good diversity performance.

Table 4. Simulated MEG for the proposed 4-port MIMO antenna.

Frequency [GHz]	Mean Effective Gain [dB]	
	Antenna 1	Antenna 3
26.0	-3.79295	-3.54989
26.5	-3.64159	-3.49506
27.0	-3.40630	-3.35325
27.5	-3.22837	-3.23593
28.0	-3.20150	-3.18450
28.5	-3.25577	-3.23715
29	-3.34699	-3.33298

## 5. COMPARISON WITH RELATED WORK

The comparison of the proposed MIMO antenna with existing antennas has been delineated with existing antennas in Table 1. It can be seen from this table that the proposed antenna has a broad frequency response, as the range it is intended to operate within is relatively wide and encompasses a large range of frequencies around the center frequency, except [4, 6, 8, 18]. If we visualize antenna in [4], its size is larger along with low isolation

when compared to the proposed antenna. Antennas in [6, 8] occupy a small size and exhibit a higher gain. However, they both offer higher ECC, which leads to higher mutual coupling in comparison with the proposed design of this work. Antennas in [18] provides a gain of 4.583 dBi, which is smaller than the one obtained by the use of the proposed structure. Moreover, It can be noticed that our work outperforms the proposed MIMO antenna in [5] in terms of size, gain, isolation, ECC, and bandwidth. Despite that, our work has a smaller gain than that in [7]; it provides a wider bandwidth and high isolation over the first band. While antennas in [16, 19] have a smaller physical footprint compared to our work; it does not offer satisfactory results in terms of other performance metrics. The designs in [17, 20] have good isolation but they are both narrower in bandwidth than the design proposed in this paper. Moreover, the design in [20] has a larger size. It can be inferred that the proposed design offers satisfactory performance with a low profile and simple structure. The integration of a decoupling structure (DGS) in a limited space greatly reduces the coupling between the antennas, which results in improved performance of the proposed design.

## 6. COMPARISON WITH CST

Using CST, we performed a comparative simulation of the reflection coefficient  $S_{11}$  parameters. Fig. 10 shows that the simulated  $S_{11}$  results in CST are in excellent agreement with the simulated  $S_{11}$  results obtained from HFSS. This result is carried out in order to validate the results obtained by the proposed antenna discussed before.

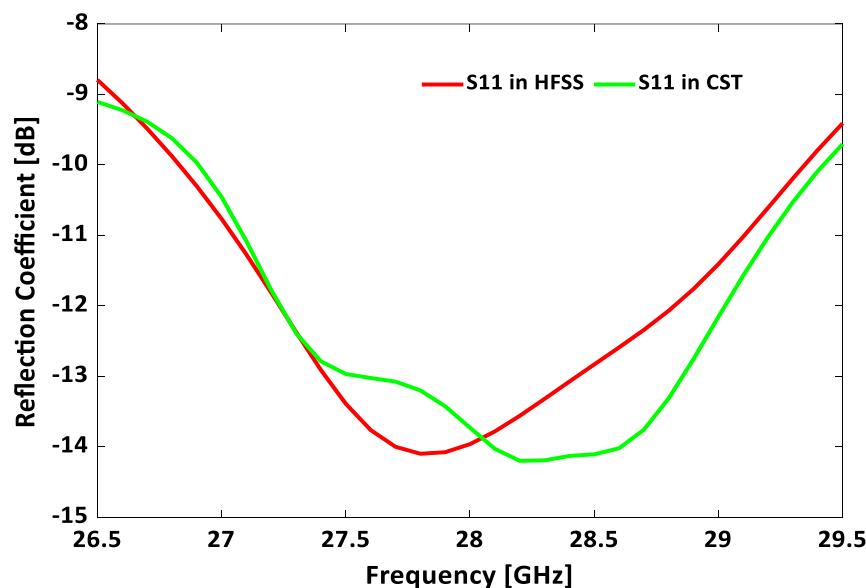


Fig. 10. Simulated  $S_{11}$  using CST.

## 7. CONCLUSIONS

In order to support 5G IoT applications, a four-port MIMO array antenna operating in 26.9-29.3 GHz with a modified ground structure was presented. The simulated MIMO antenna exhibited a bandwidth of 2.4 GHz, a peak gain of 5.25 dBi, and high isolation levels greater than 27 dB. These results were obtained due to the suggested geometrical modification in the structure. To assess the MIMO effectiveness, ECC, DG, CCL, TARC and MEG MIMO diversity calculations were performed. The findings supported the intended

performance of the suggested MIMO structure. Hence, the proposed MIMO antenna proved to be useful in 5G applications especially at 27.7 GHz and can be deployed in both American and Japanese bands, i.e., 27.5-28.35 GHz and 27.5-28.28 GHz, respectively.

## REFERENCES

- [1] M. Sangwan, G. Panda, P. Yadav, "A literature survey on different MIMO patch antenna," *In 2020 International Conference on Inventive Computation Technologies*, pp. 912-918, 2020.
- [2] J. Mestoui, M. El Ghzaoui, M. Fattah, A. Hmamou, J. Foshi, "Performance analysis of CE-OFDM-CPM Modulation using MIMO system over wireless channels," *Journal of Ambient Intelligence and Humanized Computing*, vol. 11, pp. 3937-3945, 2020.
- [3] M. El Ghzaoui, A. Hmamou, J. Foshi, J. Mestoui, "Compensation of non-linear distortion effects in MIMO-OFDM systems using constant envelope OFDM for 5G applications," *Journal of Circuits, Systems and Computers*, vol. 29, no. 16, pp. 205-257, 2020.
- [4] M. Khodeir, S. Alquran, "Secrecy performance for underlay cooperative cognitive radio network with energy harvesting and transmit antenna selection using MIMO over Nakagami-m fading channels," *Jordan Journal of Electrical Engineering*, vol. 7, no. 4, pp. 360-376, 2021.
- [5] D. Wen, Y. Hao, H. Wang, H. Zhou, "Design of a MIMO antenna with high isolation for smartwatch applications using the theory of characteristic modes," *IEEE Transactions on Antennas and Propagation*, vol. 67, no. 3, pp. 1437-1447, 2018.
- [6] A. Farahat, K. Hussein, "28/38 GHz dual-band Yagi-Uda antenna with corrugated radiator and enhanced reflectors for 5G MIMO antenna systems," *Progress In Electromagnetics Research C*, vol. 101, pp. 159-172, 2020.
- [7] B. Aghoutane, S. Das, M. Ghzaoui, B. Madhav, H. El Faylali, "A novel dual band high gain 4-port millimeter wave MIMO antenna array for 28/37 GHz 5G applications," *AEU-International Journal of Electronics and Communications*, vol. 145, pp. 154071, 2022.
- [8] M. Khalid, S. Iffat Naqvi, N. Hussain, M. Rahman, S. Fawad Mirjavadi, M. Khan, Y. Amin, "4-Port MIMO antenna with defected ground structure for 5G millimeter wave applications," *Electronics*, vol. 9, no. 1, pp. 71, 2020.
- [9] P. Liu, X. Zhu, Y. Zhang, X. Wang, C. Yang, Z. Jiang, "Patch antenna loaded with paired shorting pins and H-shaped slot for 28/38 GHz dual-band MIMO applications," *IEEE Access*, vol. 8, pp. 23705-23712, 2020.
- [10] K. Mahmoud, A. Montaser, "Synthesis of multi-polarised upside conical frustum array antenna for 5G mm-Wave base station at 28/38 GHz," *IET Microwaves, Antennas and Propagation*, vol. 12, no. 9, pp. 1559-1569, 2018.
- [11] B. Aghoutane, M. El Ghzaoui, S. Das, W. Ali, H. El Faylali, "A dual wideband high gain 2x2 multiple-input-multiple-output monopole antenna with an end-launch connector model for 5G millimeter-wave mobile applications," *International Journal of RF and Microwave Computer-Aided Engineering*, vol. 32, no. 5, pp. e23088, 2022.
- [12] P. Njogu, B. Sanz-Izquierdo, A. Elibiary, S. Jun, Z. Chen, D. Bird, "3D printed fingernail antennas for 5G applications," *IEEE Access*, vol. 8, pp. 228711-228719, 2020.
- [13] Y. Sun, D. Wu, X. Fang, N. Yang, "Compact quarter-mode substrate-integrated waveguide dual-frequency millimeter-wave antenna array for 5G applications," *IEEE Antennas and Wireless Propagation Letters*, vol. 19, no. 8, pp. 1405-1409, 2020.
- [14] N. Hussain, W. Awan, W. Ali, S. Naqvi, A. Zaidi, T. Le, "Compact wideband patch antenna and its MIMO configuration for 28 GHz applications," *AEU-International Journal of Electronics and Communications*, vol. 132, pp. 153612, 2021.

- [15] R. Chandra, D. Sarkar, D. Ganguly, C. Saha, J. Siddiqui, Y. Antar, "Design of NFRP based SIR-loaded two element MIMO antenna system for 28/38 GHz sub mm-wave 5G applications," *In 2020 IEEE 3rd 5G World Forum*, pp. 514-518, 2020.
- [16] S. Pandit, A. Mohan, P. Ray, B. Rana, "Compact four-element MIMO antenna using DGS for WLAN applications," *In 2018 International Symposium on Antennas and Propagation*, pp. 1-2, 2018.
- [17] K. Malaisamy, M. Santhi, S. Robinson, "Design and analysis of 4× 4 MIMO antenna with DGS for WLAN applications," *International Journal of Microwave and Wireless Technologies*, vol. 13, no. 9, pp. 979-985, 2021.
- [18] P. Sharmaa, T. Khanb, "A compact MIMO antenna with DGS structure," *International Journal of Current Engineering and Technology*, vol. 3, no. 3, pp. 780-782, 2013.
- [19] S. Pandit, P. Ray, A. Mohan, "Compact MIMO antenna enabled by DGS for WLAN applications," *In 2018 IEEE International Symposium on Antennas and Propagation and USNC/URSI National Radio Science Meeting*, pp. 35-36, 2018.
- [20] M. Sufian, N. Hussain, A. Abbas, J. Lee, S. Park, N. Kim, "Mutual coupling reduction of a circularly polarized MIMO antenna using parasitic elements and DGS for V2X communications," *IEEE Access*, vol. 10, pp. 56388-56400, 2022.
- [21] R. Chatterjee, *Antenna Theory and Practice*, New Age International, 1996.